PHYSICAL REVIEW E **72**, 035302(R) (2005)

Large-scale intermittency in two-dimensional driven turbulence

Yonggun Jun and X. L. Wu
Department of Physics, University of Pittsburgh, Pittsburgh, Pennsylvania 15260, USA
(Received 14 March 2005; published 16 September 2005)

It is generally believed that two-dimensional turbulence is immune to intermittency possibly due to the absence of vortex stretching. However, in turbulence created in a freely suspended soap film by electromagnetic forcing, it is found that intermittency is not insignificant. We draw this conclusion based on the measured velocity structure function $S_p(l)(\equiv\langle|\delta v_l|^p\rangle)\propto l^{\zeta_p}$ on scales l greater than the energy injection scale l_{inj}. The scaling exponent ζ_p vs p deviates from the expected linear relation and shows intermittent behavior comparable to that observed in fully developed three-dimensional turbulence in wind tunnels. Our measurements demonstrate that intermittency can be accounted for by the nonuniform distribution of saddle points in the flow.

DOI: 10.1103/PhysRevE.72.035302 PACS number(s): 47.27.Ak, 47.27.Gs, 47.27.Jv, 47.53.+n

Existing experiments and theory suggest that two-dimensional (2D) turbulence on large scales represents a peculiar state of matter that is not far from thermal equilibrium. This is surprising because the system is dissipative and strongly driven by an external source. The experimental evidence derives from the remarkable observation of Paret and Tabeling, who showed that in 2D turbulence created in a shallow layer of electrolyte, the energy spectrum $E(k)$ exhibits a $k^{-5/3}$ law, whereas the probability density function (PDF) $P(\delta v_l)$ of the velocity difference on scales l is, to a good approximation, a Gaussian function [1]. This measurement suggests that the energy transfer rate, which is proportional to the skewness of $P(\delta v_l)$, is weak compared to its three-dimensional (3D) counterparts and may be the cause of weak intermittency. It has been recently postulated by L'vov *et al.* [2] that this interesting behavior may be intimately connected with the presence of a special dimension ($d_C=4/3$) in which the $k^{-5/3}$ law holds but the enstrophy flux is strictly zero. Thus, the dynamics of the system are governed by the equipartition of enstrophy. They further demonstrated that $d=2$ is not too remote from d_C and the Gaussian statistics still prevail. It thus comes as a surprise that in a 2D soap film driven by electromagnetic forcing, the intermittency is not negligible as anticipated. If we characterize the strength of intermittency in terms of $\mu(\equiv 2\zeta_3-\zeta_6)$, μ is only a factor of 2 smaller than in fully developed 3D turbulence [3]. Here ζ_p is defined by the *pth*-order longitudinal velocity structure function $S_p(l)(=\langle|\delta v_l|^p\rangle\equiv\langle|[\vec{v}(\vec{x}+\vec{l})-\vec{v}(\vec{x})]\cdot\hat{l}|^p\rangle)\propto l^{\zeta_p}$. In an effort to identify the source of intermittency, $S_p(l)$ is compared with the moments of the coarse-grained energy dissipation rate ε_l^{dis} on scales l using the Kolmogorov refined similarity hypothesis (K62) [4]. It is unclear at the outset whether K62 is applicable to 2D turbulence on large scales because the energy transfer mechanism in 2D is entirely different from that in 3D. However, our measurements show that K62 in its original form works rather well for all moments up to $p=9$. This implies that the coarse-grained energy transfer rate ε_l^t is proportional to ε_l^{dis} in the inertial range ($l_{inj}\leqslant l\leqslant l_o$), and both are connected with the saddle structures in the flow. Here l_{inj} and l_o are the energy injection and the outer scale of turbulence.

The experiment was carried out in a freely suspended horizontal soap film (7×7 cm^2) driven by electromagnetic forcing. The v_{rms} is $\sim$12 cm/s with the Taylor microscale Reynolds number $\mathrm{Re}_\lambda\simeq 170$. The film is supported by a square plastic frame with two opposite sides made of metal electrodes. The film is placed $\sim$1 mm above a set of bar magnets of alternating poles, which creates a one-dimensional (1D) period magnetic field $[B_z(x)=B_0\sin(\pi x/a)]$ normal to the film plane, where $a=0.25$ cm is the width of a magnet. The electrodes allow a uniform current I to be injected into the film, resulting in a spatially periodic force field $F_y=F_{y0}\sin(\pi x/a)$. To minimize hydrolysis, the direction of I is switched at a fixed frequency f. A computer-controlled feedback system allows the film thickness ($h\simeq 50$ μm) and film-magnet distance to be maintained [5]; the latter determines the linear damping force $-\alpha\vec{v}$ on the film. The soap solution is made of distilled water (400 ml), detergent Dawn (5 ml), glycerol (50 ml), and ammonium chloride salt (80 g). Hollow glass beads (diam $\simeq 10$ μm) serve as tracers for the velocity measurement. For small I, the base flow is a set of shear bands, known as the Kolmogorov flow. The primary instability, when I increases, is a set of vortices on a triangular lattice with the nearest spacing of $2a/\sqrt{3}=0.29$ cm, which sets the scale of energy injection l_{inj}. Particle imaging velocimetry (PIV) was used to measure the velocity field at a rate of 15 fps, and each velocity field contains $>2\times 10^4$ vectors. The charged-coupled device (CCD) camera (PIV-CAM 10-30, TSI) used consists of 1000×1000 pixels, which maps to a 4.5×4.5 cm^2 area.

Figure 1(a) shows an overlaid image of the velocity $\vec{v}(\vec{x})$ and the enstrophy $\omega(\vec{x})^2=\Sigma_{i,j}(\partial_i v_j-\partial_j v_i)^2/2$ fields. An interesting feature of the image is that the enstrophy is concentrated in patches, and strong long-lived vortices are nearly axially symmetric. The weak vortices, on the other hand, are susceptible to be torn by the straining motion of the flow and are elongated. Figure 1(b) is for the same $\vec{v}(\vec{x})$ field, but the squared strain rate or the saddle point $\sigma(\vec{x})^2=\sigma_{i,j}(\partial_i v_j+\partial_j v_i)^2/2$ is plotted. By definition, the local fluid viscous dissipation is given by $\varepsilon^{dis}(\vec{x})=\nu\sigma(\vec{x})^2$, where ν is the viscosity of the film. The figure shows that the distribution of $\sigma(\vec{x})^2$ is different from that of $\omega(\vec{x})^2$; the saddles are more connected and populated between vortices. An ensemble of $\vec{v}(\vec{x})$ such as this one allows us to calculate various statistical

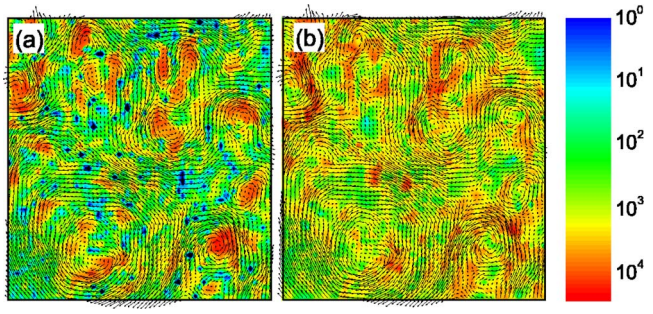

FIG. 1. (Color online) (a) The velocity $\vec{v}(\vec{x})$ and the enstrophy $\omega^2(\vec{x})$ fields. (b) The velocity and the square of strain $\sigma^2(\vec{x})$ fields. The image size is 4×4 cm^2.

quantities of 2D turbulence. Of particular interest is the velocity structure function $S_p(l)$ and its relation to the locally averaged saddles or equivalently the local dissipation rate,

$$\varepsilon_l^{dis}(\vec{x}) \equiv \frac{4}{\pi l^2}\int_{|\vec{x}-\vec{x}'|\le l/2} \varepsilon^{dis}(\vec{x}')d\vec{x}'. \quad (1)$$

Among different moments, $S_2(l)$ and $S_3(l)$ hold a special significance. The second moment represents the energy distribution on different scales. In our experiment, the shape of $S_2(l)$ is sensitive to the forcing frequency, possibly due to a competition between time scales of forcing and the energy transfer. For high frequencies ($f \geqslant 3$ Hz), $S_2(l)$ is not a power law of l for $l > l_{inj}$, regardless of the magnitude of forcing. For lower frequencies ($f \sim 1$ Hz), on the other hand, a limited scaling range emerges. Figure 2(a) displays the measurements with $f=3$ (circles, $\mathrm{Re}_\lambda=79.9$) and 1 Hz (squares, $\mathrm{Re}_\lambda=166.9$), respectively. One observes that although both data display a well-developed enstrophy subrange, $S_2(l) \propto l^{1.9\pm0.1}$, the large-scale behavior is entirely different. For 1 Hz, $S_2(l) \propto l^{2.3/3}$ over about a half decade in l. The scaling exponent is 15% greater than the theoretically predicted 2/3 and was found to depend on Re_λ systematically, i.e., $\zeta_2 \simeq 0.67\pm0.07$ for $\mathrm{Re}_\lambda=110.3$ and increases to $\zeta_2 \simeq 1\pm0.1$ for $\mathrm{Re}_\lambda=212.1$. Similar to $S_2(l)$, the third moment $S_{(3)}(l)$ was

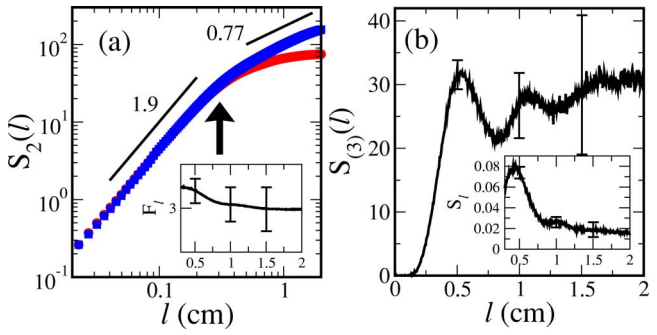

FIG. 2. (Color online) (a) The second-order structure function $S_2(l)$ measured with $f=1$ Hz (squares, $\mathrm{Re}_\lambda=166.9$) and 3 Hz (circles, $\mathrm{Re}_\lambda=79.9$). The injection scale l_{inj} is marked by the vertical arrow and the outer scale $l_o \simeq 2$ cm. The inset is the flatness F_l at 1 Hz. (b) The third-order structure function $S_{(3)}(l)$ with $\mathrm{Re}_\lambda=166.9$ and $f=1$ Hz. The inset is the skewness S_l.

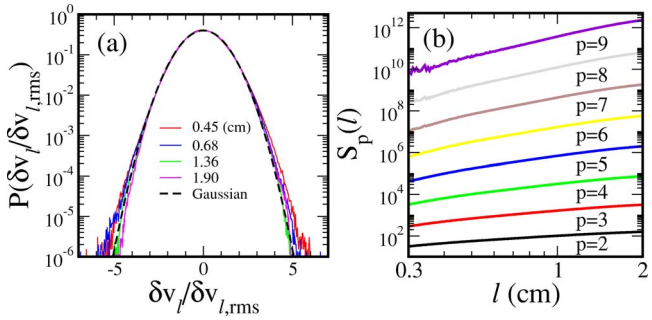

FIG. 3. (Color online) (a) The normalized PDFs of δv_l for various scales. (b) $S_p(l)$ vs l.

also found to deviate from the theoretical prediction as delineated in Fig. 2(b), where the subscript (3) stands for the moment calculated *without* the absolute sign. Here one observes that $S_{(3)}(l)$ is not linear in l but oscillates in space due to the spatially periodic forcing in the experiment. This spatial anisotropy, however, was not observed in the even moments $S_p(l)$. For all scales, $S_{(3)}(l)$ is positive, showing that the direction of energy transfer is from small to large scales and is consistent with the inverse energy cascade of 2D turbulence. For the rest of this paper, we will concentrate on the data set taken with $f=1$ Hz and $\mathrm{Re}_\lambda=166.9$.

In Fig. 3(a), the normalized PDF of δv_l on various scales $l=0.45$, 0.68, 1.36, and 1.90 cm are plotted. As can be seen, the center part of the PDFs can be fitted well by a Gaussian distribution function (the dashed line), but systematic deviations are found in the wings of the PDFs, particularly for small l. Each PDF consists of more than 5×10^6 data points and the size of the data sets is thus comparable to the 3D experiment [3]. Using the ranking order or the Zipf distribution of δv_l [6], it is possible to estimate the highest moment p_{max} that can be calculated from a given data set. In our case, p_{max} turns out to be ~9, which is smaller than $p_{max}=12$ [1] and 14 [3] in earlier works. Figure 3(b) displays a set of $S_p(l)$ for $l > l_{inj}$. As shown, all moments scale as $S_p(l) \propto l^{\zeta_p}$. Although the scaling range is limited, the exponents ζ_p nonetheless can be extracted from the slopes of the individual curves. This is delineated as diamonds in the inset (a) of Fig. 4. If 2D turbulence is nonintermittent as suggested, ζ_p would be a linear function of p. This is clearly not the case in our experiment; ζ_p bends for $p>4$ and its initial slope of 1.18/3 is greater than 1/3 as shown by the solid line. The bending of ζ_p indicates that the velocity field in soap-film turbulence is intermittent, and the large initial slope suggests that the Kolmogorov-like scaling cannot apply to our system. To compare our experiment with previous investigations [1,3], the relative scaling exponents

$$\overline{\zeta_p/\zeta_3}\left(=\overline{\frac{d\ln[S_p(l)]}{d\ln(l)} \Big/ \frac{d\ln[S_3(l)]}{d\ln(l)}}\right)$$

are plotted as squares in Fig. 4, where the overbvar represents the average over the inertial range. By plotting the ratio of the derivatives as a function of l,

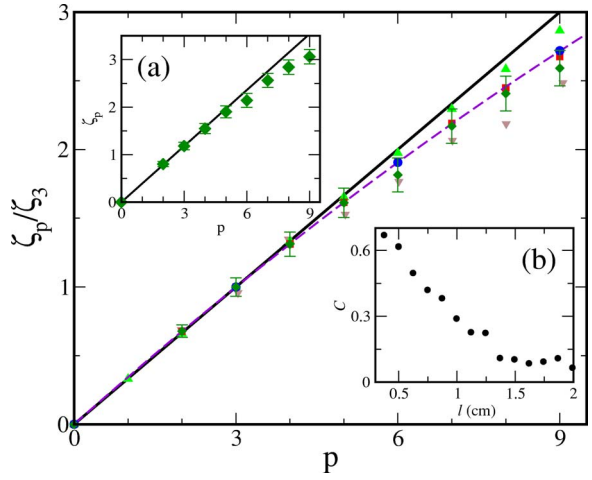

FIG. 4. (Color online) The main figure shows that (i) the relative scaling exponents ζ_p/ζ_3 (diamonds) and $\overline{\zeta_p/\zeta_3}$ (squares) measured using different methods are consistent, (ii) ζ_p/ζ_3 are also consistent with the local energy dissipation rate measurements $\phi(p)$ (circles), and (iii) the intermittency in the film is stronger than that seen in Ref. [1] (triangles) but weaker than in Ref. [3] (down triangles). The solid line is for $\zeta_p/\zeta_3=p/3$ and the dash line is the logarithmic normal-model fit to our data ($\mu\sim 0.11$). Inset (a) displays ζ_p measured directly from the slopes of the data sets on Fig. 3(b). Inset (b) displays the correlation coefficients between $|\widetilde{\delta v_l}|$ and ε_l^ν in the inertial range.

$$\frac{d\ln[S_p(l)]}{d\ln(l)} \Big/ \frac{d\ln[S_3(l)]}{d\ln(l)}$$

was found to be constant over a broader range of l and its averaged value $\overline{\zeta_p/\zeta_3}$ could be better determined than individual ζ_p [7]. In this experiment, however, we found that the two methods yield essentially the same result, i.e., $\overline{\zeta_p/\zeta_3} \simeq \zeta_p/\zeta_3$, as evidenced by the closeness of squares and diamonds in the main figure. In Fig. 4 we also plot the data for fully developed 3D turbulence (down triangles) measured by Anselmet *et al.* [3] and the 2D data (triangle) by Paret [1]. As will be shown below, if K62 is valid and ε_l obeys a logarithmic-normal distribution [8], the relative scaling exponent ζ_p/ζ_3 can be calculated explicitly with the result $\zeta_p/\zeta_3=p/3+(\mu/18\zeta_3)(3p-p^2)$, where $\mu(=2\zeta_3-\zeta_6)$ characterizes the width of the distribution of ε_l and is the only adjustable parameter. For our experiment, a fitting procedure yielded $\mu\simeq 0.11$. This value should be compared with $\mu \simeq 0.2$ for the 3D turbulence data [3] and $\mu\simeq 0.03$ for Paret's data [1].

Despite the intermittency for large p, the low-order statistics observed in our experiment are in reasonably good agreement with Paret's measurements [1] and with the numerical simulation [9]. For instance, (i) the overall skewness $S_l=S_{(3)}(l)/S_2(l)^{3/2}$ displayed in the inset of Fig. 2(b) is rather small; it is $\sim 8\%$ near l_{inj} and decreases to $\sim 2\%$ for large scales. The averaged value in the inertial range is $\bar{S}=0.03\pm 0.02$. This is to be compared with the skewness of 5% seen in Paret's experiment and 3% in the simulation. (ii) Similar to S_l, the flatness $F_l=S_4(l)/S_2(l)^2$ in the inset of Fig. 2(a) is not constant but varies from 3.25 near l_{inj} to 3.0 for large scales. The average value $\bar{F}=3.1$ agrees well with the Gaussian value of 3. It should be emphasized that although $\bar{S}$ and $\bar{F}$ are reasonably consistent with the Gaussian statistics, it does not imply that higher order statistics need to be so. As the order p increases, rare events associated with the tails of the PDFs [see Fig. 3(a)] become more prominent. Since these rare events are l dependent, ζ_p must be a nonlinear function of p.

We next turn our attention to find whether the observed intermittency can be accounted for in a similar fashion as K62 [4]. This hypothesis has been the cornerstone for understanding 3D turbulence, and it would be interesting to see if this important idea has any relevance to 2D turbulence. The basic observation in 3D turbulence is that velocity fluctuations possess a broad spectrum and that the globally averaged energy dissipation rate ε cannot account for rare, intense local fluctuations. One way to fix this statistical bias is to divide the spatial domain into a collection of ensembles of size l, each characterized by a locally averaged energy dissipation rate $\varepsilon_l(\vec{x})$ as defined in Eq. (1). It was conjectured by Kolmogorov that for the inertial range of scales, the PDF of the stochastic variable $V=\delta v_l/(l\varepsilon_l)^{1/3}$ depends only on the local Reynolds number $\mathrm{Re}_l=\langle l(l\varepsilon_l)^{1/3}\rangle_l/\nu$ and in the limit $\mathrm{Re}_l\gg 1$, the PDF is universal, independent of Re_l. If one further assumes the statistical independence between the random variables V and $(l\varepsilon_l)^{1/3}$ [10], it follows that $S_p(l) \equiv\langle \delta v_l^p\rangle=\langle V^p\rangle\langle\varepsilon_l^{p/3}\rangle l^{p/3}=C_p l^{p/3+\tau_{p/3}}=C_p l^{\zeta'_p}$, where C_p is a p-dependent constant, $\langle\varepsilon_l^p\rangle\propto l^{\tau_p}$ and $\zeta'_p=p/3+\tau_{p/3}$. Thus, if K62 is valid, one expects $\zeta_p=\zeta'_p$ for all p. By using the ratio of moments $S_p(l)/S_3(l)^{p/3}$ instead of the moment itself, the K62 can be generalized and facilitates a better determination of scaling exponents. This is the essence of extended self-similarity and has been successfully applied to turbulence with a low Re or with a nonclassical exponent ($\zeta_3\neq 1$) [11]. It is readily shown $\zeta_p/\zeta_3=p/3+\tau^*_{p/3}/\zeta_3$, where $\tau^*_{p/3}=\tau_{p/3}-(p/3)\tau_1$. If ε_l is distributed in a logarithmic-normal fashion, $\tau_1=0$ and $\tau^*_{p/3}=\tau_{p/3}=(\mu/18)(3p-p^3)$, where μ is the width of the $\ln(\varepsilon_l)$ distribution [8]. The above discussion shows that the reason ζ_p deviates from the linear p dependence is because of the nontrivial distribution of ε_l characterized by $\tau_{p/3}$. It should be emphasized that though K62 has gained considerable experimental and numerical support for 3D turbulence [10,12–14], its implication for 2D turbulence remains unclear and is analyzed below.

A difficulty in applying K62 to 2D turbulence is that energy dissipation due to the fluid viscosity $\varepsilon_l^{dis}=\varepsilon_l^\nu[\equiv\nu\langle\sigma(\vec{x}')^2\rangle_l]$ may not be entirely relevant to large-scale velocity fluctuations because energy flux is reversed. To our surprise, however, we found that δv_l and ε_l^ν are strongly correlated in soap films. The coefficient of correlation $C(l)=\langle[|\delta\widetilde{v_l(\vec{x})}|-\langle|\delta\widetilde{v_l(\vec{x})}|\rangle]\cdot[\varepsilon_l^\nu(\vec{x})-\langle\varepsilon_l^\nu(\vec{x})\rangle]\rangle/(s_{|\widetilde{\delta v_l}|}s_{\varepsilon_l^\nu})$ is plotted in the inset (b) of Fig. 4, where $\delta\widetilde{v_l(\vec{x})}$ is the averaged longitudinal velocity difference on the circumference of a randomly selected disk of diameter l, $\varepsilon_l^\nu(\vec{x})$ is the viscous dissipation inside the disk, $s_{|\widetilde{\delta v_l}|}$ and $s_{\varepsilon_l^\nu}$ are their standard deviations, and the angular bracket is the volume plus the

time average. We observed that the correlation is about 70% near l_{inj} and decreases to about 10% for large l. This degree of correlation is in par with what was observed in the inertial range of 3D turbulence [10,12–14]. We next proceeded to calculate energy dissipation statistics within disks of diameter l. The coarse-grained values of $\varepsilon_l^{dis}(\vec{x})$ are calculated according to Eq. (1) and the scaling exponents τ_p^* are evaluated based on an ensemble of disks. The resulting exponents, $\phi(p) \equiv p/3 + \tau_{p/3}^*/\zeta_3$, can thus be compared with the relative exponents ζ_p/ζ_3 calculated using δv_l. As shown by the solid circles in Fig. 4, the scaling exponents $\phi(p)$ are nearly identical to ζ_p/ζ_3, indicating that intermittency in δv_l are consistent with the nonuniform distribution of ε_l^{dis}. For completeness, we also included the air drag $\varepsilon_l^{\alpha} \equiv \alpha \langle \vec{v}(\vec{x})^2 \rangle_l$ in the energy dissipation, $\varepsilon_l^{dis}(\vec{x}) = \varepsilon_l^{\nu}(\vec{x}) + \varepsilon_l^{\alpha}(\vec{x})$. Here we found that the scaling exponents τ_p^* are unaffected by the air contribution (data not shown), suggesting that intermittency observed in this experiment is due almost entirely to ε_l^{ν}. The weak air contribution is expected in the inertial range and is consistent with our earlier findings that air drag is significant only for $l > l_0$ [5].

It remains to be clarified the striking fact that the relative scaling exponent ζ_p/ζ_3 can be accounted for by the intermittency in the locally averaged dissipation field $\langle (\varepsilon_l^{dis})^{p/3} \rangle \propto l^{\tau_{p/3}}$ with the result $\zeta_p/\zeta_3 \simeq p/3 + [\tau_{p/3} - (p/3)\tau_1]/\zeta_3$. The finding is surprising because in 2D turbulence most of injected energy is transferred to large l instead of being dissipated in small l. Thus, the scaling behavior for the velocity difference δv_l on large scales should be determined by the energy transfer rate ε_l^t rather than the local energy dissipation rate ε_l^{dis}. However, using the Navier-Stokes equation with a forcing term $\vec{F}$, it can be shown that the energy transfer rate to large scales is given by $\varepsilon_l^t = \varepsilon_l^{inj} - \varepsilon_l^{dis}$, where $\varepsilon_l^{inj} = \langle \vec{F}(\vec{x}) \cdot \vec{v}(\vec{x}) \rangle_l$ is the energy injection rate averaged over l. This energy budget is exact scale by scale. In particular, in the inertial range ($l_{inj} \leqslant l \leqslant l_0$), one expects $\varepsilon_l^t > 0$. Our observed scaling behavior therefore demands ε_l^t to be proportional to ε_l^{dis} or $\varepsilon_l^t = A\varepsilon_l^{dis}$, where $A > 0$ is a constant. In light of the energy budget, $\varepsilon_l^{inj} = (A+1)\varepsilon_l^{dis}$ in the inertial range. The above proportionalities ($\varepsilon_l^t \propto \varepsilon_l^{dis} \propto \varepsilon_l^{inj}$) make physical sense, and they imply that regions of large energy injection would on average dissipate more energy on small scales and at the same time transfer more energy to large scales. Indeed in 2D turbulence, longitudinal velocity fluctuations δv_l were found to correlate strongly with saddle points $\sigma^2(\vec{x})$ in the flow [15], which are responsible for energy dissipation as well as for energy transfer to large scales. In a recent study, we also found that when saddles are suppressed by polymers, inverse energy cascade is terminated [16]. Thus, even though turbulence in 2D and 3D is very different, both in hydrodynamic structures and in the mechanism of energy transfer, Kolmogorov's central idea of cascade, i.e., a dynamic equilibrium of energy flux $\delta v_l^3/l$ through fluctuations of size l and energy dissipation ε_l^{dis} within it, is remarkably preserved in two dimensions.

To summarize, we found velocity fluctuations in the inverse-energy-cascade subrange to be intermittent in 2D flowing soap films. The intermittency correlates strongly with coarse-grained saddle structures in the flow (or equivalently the local viscous energy dissipation rate) in a manner similar to K62. It is unclear why our film behaves differently from previous studies [1]. One possible reason is the much higher turbulent intensity in the film than in the shallow layer of an electrolyte. The second possibility is the slight compressibility ($\sim 10\%$) of the film. These issues need to be sought out in future experiments.

We acknowledge helpful discussions with W. I. Goldburg and Jie Zhang. This work was funded by the NSF under Grant No. DMR-0242284.

[1] J. Paret and P. Tabeling, Phys. Fluids **10**, 3126 (1998).
[2] V. S. L'vov, A. Pomyalov, and I. Procaccia, Phys. Rev. Lett. **89**, 064501 (2002).
[3] A. Anselmet, Y. Gagne, R. J. Hopfinger, and R. A. Antonia, J. Fluid Mech. **140**, 63 (1984).
[4] A. Kolmogorov, J. Fluid Mech. **13**, 82 (1962).
[5] M. Rivera and X. L. Wu, Phys. Fluids **14**, 3098 (2002).
[6] T. Dudok de Wit, Phys. Rev. E **70**, 055302(R) (2004).
[7] A. Babiano, B. Dubrulle, and P. Frick, Phys. Rev. E **52**, 3719 (1995).
[8] U. Frisch, *Turbulence* (Cambridge University Press, Cambridge, 1995).
[9] G. Boffetta, A. Celani, and M. Vergassola, Phys. Rev. E **61**, R29 (2000).
[10] I. Hosokawa, C. W. Van Atta, and S. T. Thoroddsen, Fluid Dyn. Res. **13**, 329 (1994).
[11] R. Benzi, S. Ciliberto, R. Tripiccione, C. Baudet, F. Massaioli, and S. Succi, Phys. Rev. E **48**, R29 (1993).
[12] A. A. Praskovsky, Phys. Fluids A **4**, 2589 (1992).
[13] G. Stolovitzky, P. Kailasnath, and K. R. Sreenivasan, Phys. Rev. Lett. **69**, 1178 (1992).
[14] S. Chen, G. D. Doolen, R. H. Kraichnan, and Z.-S. She, Phys. Fluids A **5**, 458 (1993).
[15] W. B. Daniel and M. A. Rutgers, Phys. Rev. Lett. **89**, 134502 (2002).
[16] Y. Jun, J. Zhang, and X. L. Wu (unpublished).